

Electrical resistivity of *a*-SiC:H as a function of temperature: Evidence for discontinuities

R. Murri* and N. Pinto

INFN—Dipartimento di Matematica e Fisica, Università di Camerino, Via Madonna delle Carceri, 62032 Camerino, Italy

G. Ambrosone and U. Coscia

INFN—Dipartimento di Scienze Fisiche, Università di Napoli, Via Cintia, 80125 Napoli, Italy

(Received 28 December 1999)

We report on two different, but well defined, behaviors of resistivity vs temperature in amorphous SiC:H films deposited from (SiH₄+C₂H₂) gas mixture. The electrical resistivity shows in the range 400–500 K curves with jumps or peaks both increasing and decreasing temperature. The electrical properties of the samples are restorable even if not exactly reversible. The evolution of the structure was observed by x-ray diffraction at the beginning and at the end of the heating run. A simple phenomenological model is presented to interpret these results, introducing both the bond length and angle and their variation with temperature, in a network with a high content of voids.

Amorphous silicon carbon (*a*-SiC:H) thin films grown by plasma-enhanced chemical vapor deposition (PECVD) have been widely investigated for many electronic devices, such as window layer in solar cells,¹ insulator layer in thin film transistors,² light-emitting diodes,³ and so on.

Many papers^{4–16} are dealing with the optical and structural properties of amorphous silicon carbon and with their dependence on temperature, so giving information on thermal annealing of these physical properties. On the contrary, very few papers^{4,17,18} discuss the thermally induced changes of the electronic transport properties.

The density of defects in *a*-SiC:H films increases with the carbon content, so decreasing the photoconductivity; which can be improved with dilution of source gases with hydrogen.^{19,20}

An alternative way to improve the physical properties of the material can be the use of gas sources different from methane.²¹

Following this second way, we deposited *a*-SiC:H films starting from a gas mixture of silane and acetylene (SiH₄+C₂H₂).²² In this paper, we present a study of thermally induced reversible changes of the electrical properties in amorphous silicon carbon films. The measurements were carried out in the temperature range 300–700 K on undoped hydrogenated amorphous thin films of silicon carbon. X-ray diffraction was performed both on as-deposited and annealed samples.

We will briefly resume describing the deposition conditions and the results of the optical characterization²² of our films.

The amorphous silicon carbon films were grown in a high-vacuum PECVD system at a frequency of 13.56 MHz, changing the rf power in the range 1.5–16 W (power density: 0.01–0.1 W cm⁻²), Table I. All the films were deposited in the low power-density regime.¹⁹ The other deposition parameters were fixed as follows: electrode distance 25 mm, substrate temperature 350 °C, silane and acetylene gas flow 10.0 and 1.2 SCCM (where SCCM denotes cubic centimeter per minute at STP), respectively, and chamber pres-

sure 47 Pa. The substrates were glass (Corning 7059) and monocrystalline silicon wafers, for optical, electrical, and infrared measurements.

The refractive index and the optical gap as a function of rf power are presented in Fig. 1. Both trends, increase of *n* and decrease of *E*₀₄ as a function of rf power, are due to a decreasing incorporation of carbon in the films, with reduced nucleation of carbon clusters. IR absorption spectra of similar films, Fig. 2, show a decrease (i) of the intensities of the Si-CH_{*n*} vibrational modes at 780 cm⁻¹,² (ii) of the band 2000–2100 cm⁻¹ (attributed to stretching vibrations of SiH_{*n*} and/or C-SiH groups,^{2,21}), and (iii) of the band 2800–3000 cm⁻¹ (assigned to stretching vibrations of CH_{*n*} groups) increasing the rf power.²² The Urbach energy decreases from 92 to 60 meV, with a density of states varying from 1.5 × 10¹⁷ to 3 × 10¹⁶ cm⁻³, in the range 1.5–16 W. The increase of the refractive index and the decrease of the Urbach energy indicate that the film structure was relaxed and becomes more dense with the rf power raise.

The lowering of the carbon content in films using acetylene makes these results comparable to those found in methane-based films, under hydrogen-dilution conditions^{19,20} to preparing mixtures with silane and this seems to make it acetylene attractive. This makes interesting a more deep electrical characterization.

The electrical resistivity was measured by using an electrometer (Keithley 617) in the *V/I* configuration with an input impedance greater than 10¹⁶ Ω. Two Au contacts (5 mm apart) were evaporated onto the outer surface of the samples and thermally treated at 450 K for 1 h in an oven filled with nitrogen. Fine gold wires were soldered to Au strips by an ultrasonic welder. After this, the samples were inserted in a small furnace evacuated to ≈ 10⁻¹ Pa and equipped with a temperature controller. A completely automatic system was used to measure the resistivity as a function of the temperature. The measurements were done in two different but consecutive runs: the first one starting from room temperature (RT) and going to high temperature (heating) and the second one coming back to RT (cooling). The acquisition of the *I-V* data started only when the error on settled temperature was

TABLE I. Deposition data and some physical properties of the samples used for electrical characterization: rf power, W ; thickness, d ; optical gap, E_{04} ($\alpha=10^4 \text{ cm}^{-1}$); refractive index, n ; room-temperature dark conductivity σ_d , and photoconductivity σ_{ph} ; and r , ratio between σ_d and σ_{ph} . The fluxes of SiH_4 and C_2H_2 were kept constant to 10 and 1.2 SCCM, respectively, while the substrate temperature was fixed at 620 K.

Sample	W (W)	d (nm)	E_{04} (eV)	n	σ_d S cm^{-1}	σ_{ph} S cm^{-1}	r
248	2	1330	2.21	2.66	1.4×10^{-12}	1.75×10^{-9}	1.3×10^3
249	4	1300	2.17	2.73	1.3×10^{-12}	5.9×10^{-9}	4.6×10^3
253	6	580	2.07	2.93	2.9×10^{-13}	1.2×10^{-8}	4.2×10^4
251	8	450	1.99	2.97	2.9×10^{-12}	3.2×10^{-8}	1.1×10^4
254	12	540	1.94	3.14	8.2×10^{-12}	1.3×10^{-7}	1.5×10^4

less than ± 0.5 K. We always measured under slow heating or cooling conditions: in fact, the temperature rate can be estimated to about 2×10^{-2} K/s. Each point of the experimental resistivity curves was computed by averaging over 50 acquisitions for I , V and T .

Figures 3 and 4 show the behavior of the electrical resistivity as a function of $1/kT$ for samples deposited at 2 and 8 W, respectively (Table I). We have to note the high value of the room-temperature resistivity in all samples: it is always $> 10^8 \Omega \text{ cm}$. Choi *et al.*¹⁵ found a relation between the number of Si-H bonds ($N_{\text{Si-H}}$) and the conductivity: a higher value in $N_{\text{Si-H}}$ resulted in a lower conductivity, i.e., in a higher resistivity. According to this, our samples seem to show a high value of Si-H bonds with a low density of silicon dangling-bonds.

Two well-defined behaviors (curve with jumps or peaks) can be identified in all these measurements: to our best knowledge these are the first results ever reported in the literature for $a\text{-SiC:H}$.

We will describe in some detail the whole resistivity curve as a function of the temperature for sample 248 (Fig. 3). The first part of the resistivity curve, measured during the heating cycle (squares), has a constant behavior ($\rho \approx 9 \times 10^9 \Omega \text{ cm}$) from room temperature up to $T \approx 380$ K. Increasing T over 380 K, three well-defined jumps are clearly evident at $T \approx 435$, 440, and 490 K on the descending behavior of ρ . When T reaches ≈ 650 K ($\rho \approx 2 \times 10^4 \Omega \text{ cm}$), we started the cooling cycle, and up to $T \approx 510$ K the two ρ

curves (heating and cooling) superimpose perfectly. Still decreasing T , the resistivity curve (triangles) presents again three jumps at $T \approx 470$, 450 and 420 K. After this last jump, ρ decreases still lightly, and for $T \approx 380$ K, it superimposes perfectly to that measured during the heating.

Della Mea *et al.*⁴ presented conductivity as a function of the annealing temperature in $a\text{-Si:H}$. We replotted their data as resistivity in Fig. 3. The curve evidences the same behavior found in several of our samples. The large step of temperature increase ($\Delta T = 100$ K), could have masked the jumps, if any.

The peak-shaped behavior is shown by resistivity curves as a function of T for sample 251 (Fig. 4). Both ρ curves (heating and cooling) evidence a well-defined peak, shifted towards higher temperatures for the return (cooling) resistivity curve: ΔT is ≈ 80 – 90 K. The two curves superimpose only in the temperature range 600–750 K. The cooling curve evidences a peak for $500 < T < 600$ K and, after this, the cooling resistivity curve moves parallel to the heating one, even if with values lower by more than one and a half orders of magnitude. The room-temperature resistivity measured at the beginning of the heating run (squares) is $\rho \approx 5 \times 10^8 \Omega \text{ cm}$,

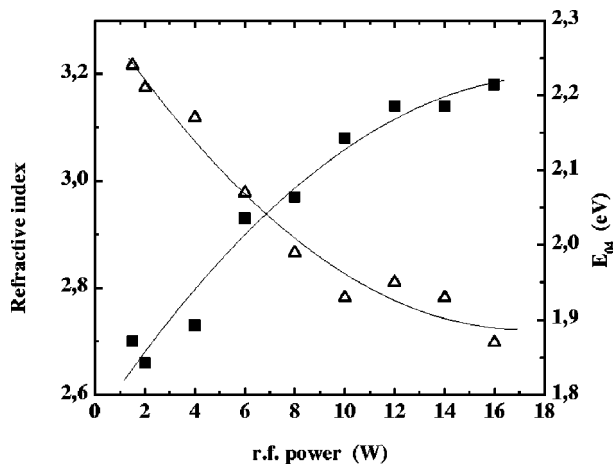


FIG. 1. Refractive index n (squares) and the optical gap E_{04} (triangles) as a function of rf power.

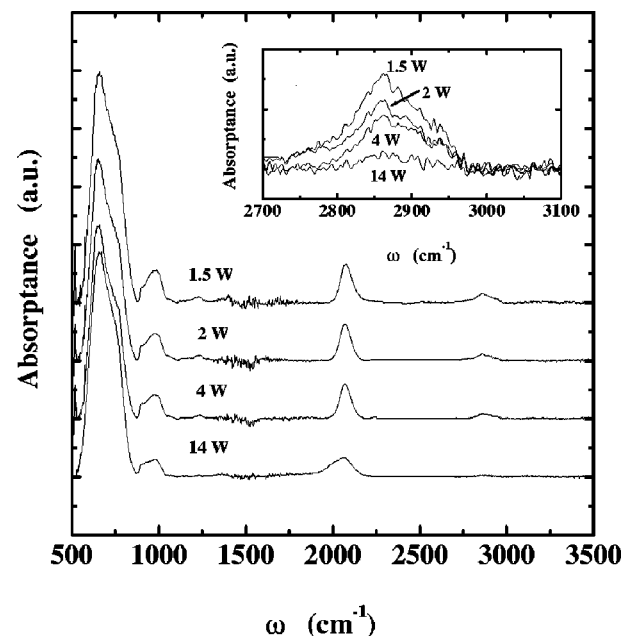


FIG. 2. IR absorption spectra for $a\text{-SiH}_{1-x}\text{C}_x$ films deposited at four different powers. The absorption region $2800\text{--}3000 \text{ cm}^{-1}$ is shown in the inset.

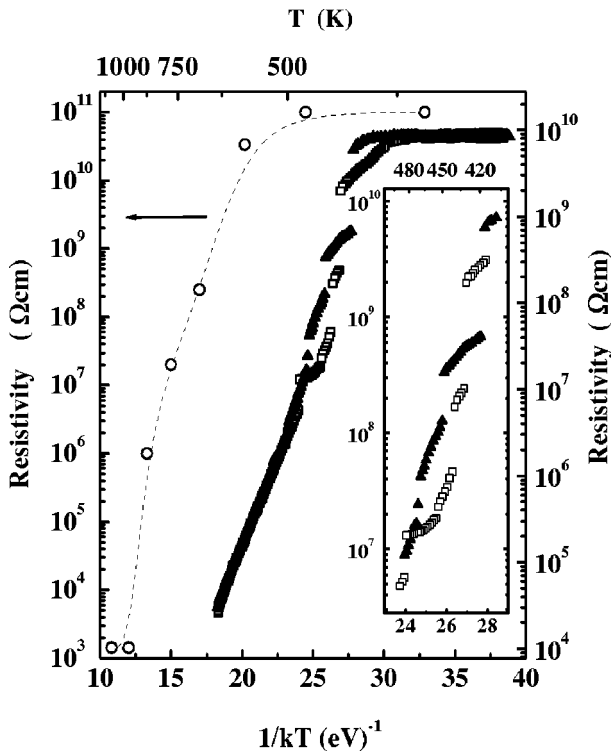


FIG. 3. Electrical resistivity as a function of temperature for sample 248 (right scale): squares are for the heating run and triangles for the cooling run. Jumps are magnified in the inset. The curve with circles is taken from Ref. 4, Fig. 6, converting data from conductivity to resistivity (left scale).

while the resistivity at the end of the cooling run is $10^7 \Omega \text{ cm}$ at $T=300 \text{ K}$.

All the other samples show similar behaviors: we found in some cases curves with jumps and others with peaks.

It was possible to define an activation energy of the conductivity, E_σ , only for $T>500-550 \text{ K}$. In all cases, E_σ

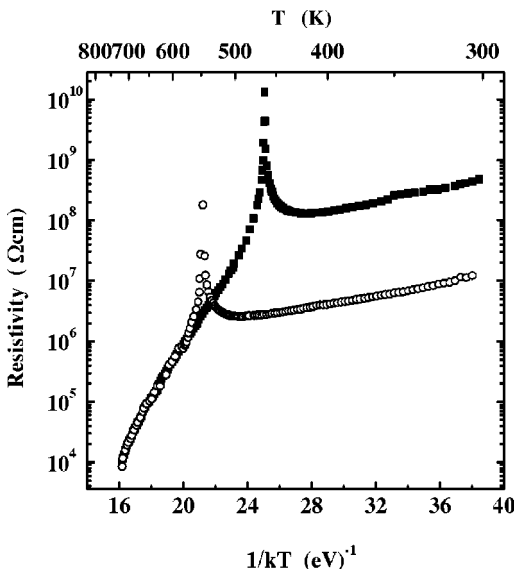


FIG. 4. Electrical resistivity as a function of temperature for sample 251: squares are for the heating run whereas circles are for the cooling run.

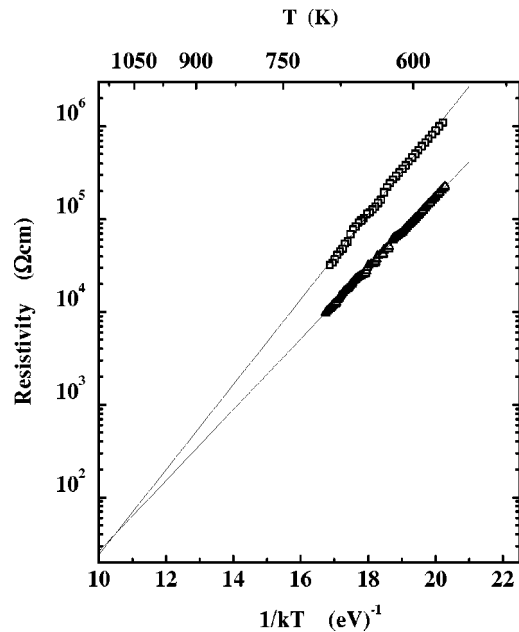


FIG. 5. Plot of the ρ points at $1/kT < 19 \text{ eV}^{-1}$: the lines are the behaviors extrapolated according to Datta.²⁴ Squares are data of Fig. 3, while triangles are those of sample 254 (not presented in the text).

ranges between 0.40 and 0.48 eV, four or five times lower than the optical gap E_{04} of the samples (Table I).

The behaviors of the resistivity curves (peak or jumps), measured as a function of the temperature, seem to imply different rearrangement mechanisms of the amorphous structure. We found, in general (i) a reversibility of the starting and of the ending parts of the resistivity curves for each sample, with two exceptions: one of these is presented in Fig. 4. However, for these two samples, if, at the end of the cooling run, we perform a thermal treatment at 550 K for 1 h, the resistivity of the sample comes back to the RT starting value of the heating run, so closing the ‘‘cycle;’’ (ii) effects of thermal hysteresis present in the central part of the curves, as shown in the inset of Fig. 3.

Do all these facts mean that the structure of the films is metastable? Does repeated thermal annealing modify the structure of the films?

We can reject the hypothesis of a possible crystallization of the structure for several reasons.

(a) The whole measuring cycle (heating and cooling) can be repeated, with the same features, many times. We verified this property in all samples: the only need is for a thermal treatment at 550 K for 1 hour before each measuring cycle;

(b) Data in the literature^{8,16} define the starting temperature for crystallization of ion-implanted *a*-SiC:H to about 1100 K or higher. The thermal treatment can only induce a rearrangement of the bonds and/or a reduction of the number of defects. Nuclear measurements⁴ and annealing of the optical properties⁵ are evidence that up to $T_A \approx 700 \text{ K}$, thermal desorption of H is very poor. Datta *et al.*²³⁻²⁵ proposed the existence of a characteristic temperature T_0 for the onset of the first stage of micro- or polycrystallization in annealed disorder-dominated systems.

We applied Datta’s method to our experimental data, plotting the resistivity as a function of the inverse annealing

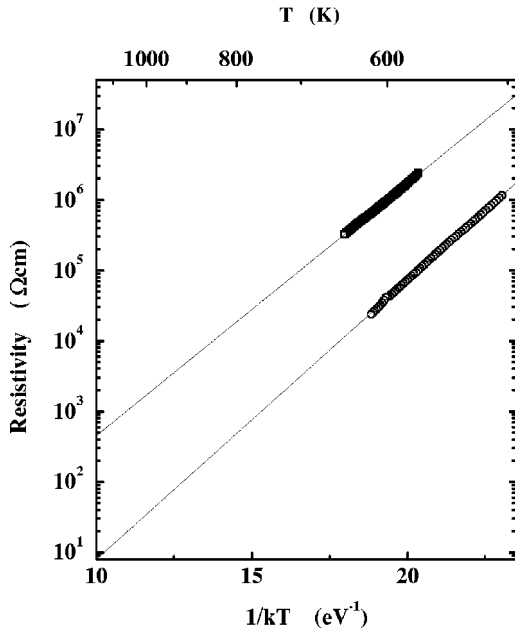


FIG. 6. Plot of the ρ points at $1/kT < 17 \text{ eV}^{-1}$: the lines are the behaviors extrapolated according to Datta.²⁴ Squares are data of Fig. 4, while circles are those of sample 253 (not presented in the text).

temperature, and then extrapolating the resistivity curves at high annealing temperature to evidence for the characteristic temperature T_0 if any (Figs. 5 and Fig. 6). The results indicate that an equilibrium temperature exists for samples for which ρ curves present peaks (Fig. 4), and it doesn't exist if jumps are present (Fig. 3). The equilibrium temperature is about 1100 K, much higher than the maximum annealing temperature (about 700 K) used in our experiments.

Zhang *et al.*⁵ quote $T_0 = T_A = 1370 \text{ K}$ as the transition temperature to microcrystallization, while El Khakani *et al.*⁶ found that annealing up to about 950 K does not influence $N_{\text{Si-C}}$, $N_{\text{Si-Si}}$, and N_{Si} , mainly due to the presence of structural disorder. Magafas⁹ from the trend of the Tauc's B parameter suggests that the structural disorder of $a\text{-SiC:H}$ is not affected by thermal annealing up to 950 K. Mencaraglia *et al.*¹⁸ in magnetron sputtered samples found a lower crystallization temperature (about 900 K).

(c) X-ray diffraction curves both for as-grown samples and at the end of the heating run were measured. The overall shapes of the spectra are similar, peaking at $2\Theta \approx 25^\circ$ with a full width at half maximum (FWHM) $\approx 7^\circ\text{--}8^\circ$, Fig. 7. Both the shift of the peak position towards lower 2Θ values, compared to crystalline SiC ($2\Theta \approx 27^\circ\text{--}28^\circ$),⁵ and the FWHM value are typical of an amorphous material. Figure 8 shows the height of the peak at $2\Theta \approx 25^\circ$ both for as-deposited and measured samples as a function of rf deposition power, W . All the curves were acquired with the same total number of counts. The height of the peak decreases linearly about 40% when W increases from 2 to 8 W, and then it is constant up to 12 W for as-grown samples. On the contrary, annealed samples evidence a peaked behavior with the maximum at 8 W.

Höfgen *et al.*²⁶ found two well-separated annealing stages in ion-implanted and -annealed samples, with $T \approx 1000 \text{ K}$ as a transition temperature between the two stages. Their

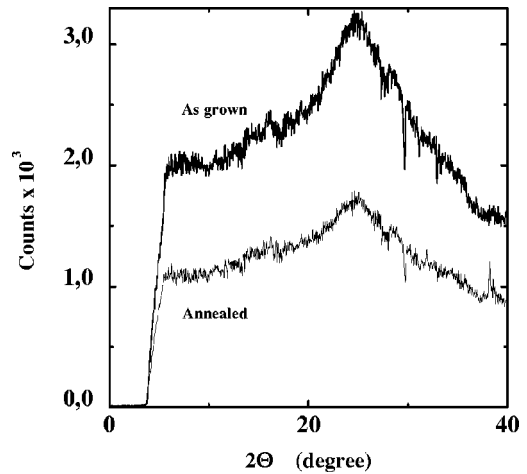


FIG. 7. X-ray diffraction curves for sample 247 in as-grown and thermally treated states.

x-ray diffraction curves for samples in the first stage of anneal are similar to ours, showing that no recrystallization hastaken place.

Furthermore, the coupling between hydrogen presence and evolution in $a\text{-SiC:H}$ films with compressive or tensile stress, respectively,¹³ cannot be considered to interpret the ρ curves. In fact, the compressive stress evolves for temperatures greater than 750–800 K, and the diffusion of hydrogen starts for $T > 900 \text{ K}$.¹⁶ Beyer *et al.*²⁷ reported on the presence of a low-temperature ($T \approx 700 \text{ K}$) exodiffusion peak of hydrogen in samples where $C > 10\%$. In our samples, due to n and E_{04} values, C ranges between 10% and 22% according to W , and the H exodiffusion temperature is very near to the upper limit of our annealing temperature. Moreover, as previously said, we have to remember that a thermal treatment at 550 K for 1 h completely restores the resistivity values. Therefore, we may exclude an exodiffusion of hydrogen.

All these experimental facts can allow, in our opinion, an explanation of the behaviors of the resistivity in terms of reversible rearrangement of the amorphous network. Lin *et al.*²⁸ using repeated thermal annealing of the infrared ab-

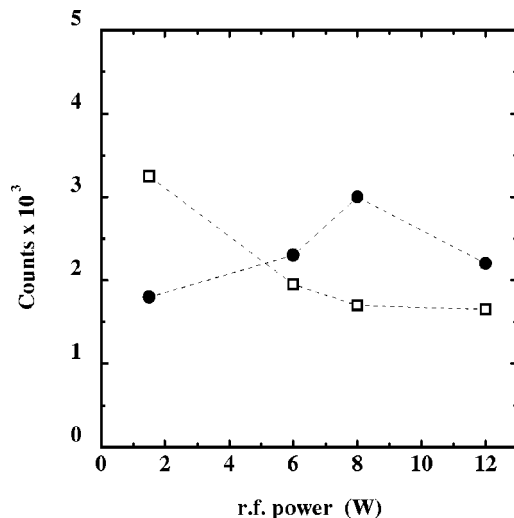


FIG. 8. Height of the peak at $2\Theta = 25^\circ$ (Fig. 7) plotted as a function of rf power for as-deposited (squares) and annealed (circles) samples.

sorption, found that a significant fraction of carbon atoms are introduced into the films in CH₃ configuration, forming local voids, polysilane chains, and dangling-bond defects. Only after high-temperature anneal are the hydrogen atoms driven out, with silicon and carbon atoms reconnected to form a better amorphous carbon network. El Khakani¹³ found that Si-H, C-H, and Si-C bond densities depend on the annealing temperatures when greater than about 800 K and the bonded hydrogen is constant up to about 900 K.

Our maximum annealing temperature was about 750 K, and the thickness of the film ranged between 0.5 and 1 μm. The fundamental point of our measurements is the complete restoring of the resistivity values. The curves are not reversible, due to the different paths for heating or cooling runs. But, we can restore the original state of the sample by doing a thermal treatment at the end of the cooling run.

A model attempting an interpretation of all these results has to consider reversible evolution of the network: in fact, as previously discussed, we have to exclude crystallization. So, we have to consider the bonds, the bond angles, and their changes as a function of the temperature in the first stage of the annealing, as defined by Höfgen.²⁶ We have also to take into account the results of Lin²⁸ about the constraint originated by the presence of CH₃ molecules for the formation of

voids in the network of *a*-SiC:H. So, we can suppose that the presence of a large number of voids allows the network to accommodate for bond length and angle variation. At the same time, hydrogen atoms can move inside the voids, only changing the decoration of the inner wall with their dangling bonds, not their density.

Our affirmations need to be supported by other measurements and structural characterizations, for example, IR absorption and x-ray diffraction performed during the temperature runs. In this way it could be possible to elucidate the nature of the jumps and peaks in the ρ curves.

In conclusion, our films, grown at low power density in the considered range of thermal annealing, maintain the amorphous structure, and the thermal treatment seems to produce only rearrangements of the bonds. The resulting structure determined by the thermal annealing is restorable eventually with a thermal treatment before starting with a new measure. A clear trend of the electrical and structural properties as a function of the carbon content cannot be evidenced, even if the value of 8 W for rf power seems to mark a possible changeover.

This work was supported by Istituto Nazionale per la Fisica della Materia (INFM).

*Email: murri@campus.unicam.it. Fax: +39 0737 632525.

¹Y. Tawada, H. Okamoto, and Y. Hamakawa, *Appl. Phys. Lett.* **39**, 237 (1981).

²A. Madan and M. P. Shaw, in *Physics and Applications of Amorphous Semiconductor* (Academic, New York, 1988), p. 149; J. Bullot and M. P. Schmidt, *Phys. Status Solidi B* **143**, 345 (1987).

³S. Nishikawa, H. Kamimura, T. Watanabe, and K. Kaminishi, *J. Non-Cryst. Solids* **59&60**, 1235 (1983).

⁴G. Della Mea, F. Demichelis, C. F. Pirri, P. Rava, V. Rigato, T. Stapinski, and E. Tresso, *J. Non-Cryst. Solids* **137&138**, 95 (1991).

⁵Fangqing Zhang, Hua Xue, Zhizhong Song, Yongping Guo, and Guanghua Chen, *Phys. Rev. B* **46**, 4590 (1992).

⁶M. A. El Khakani, D. Guay, M. Chaker, and X. H. Feng, *Phys. Rev. B* **51**, 4903 (1995).

⁷T. Friessnegg, M. Boudreau, J. Brown, P. Mascher, P. J. Simpson, and W. Puff, *J. Appl. Phys.* **80**, 2216 (1996).

⁸P. Musumeci, R. Reitano, L. Calcagno, F. Roccaforte, A. Makhataris, and M. G. Grimaldi, *Philos. Mag.* **76**, 323 (1997).

⁹L. Magafas, *J. Non-Cryst. Solids* **238**, 158 (1998).

¹⁰A. Szekeres, M. Gartner, F. Vasiliu, M. Marinov, and G. Beshkov, *J. Non-Cryst. Solids* **227&230**, 954 (1998).

¹¹A. Tabata, H. Kamijo, Y. Suzuoki, and T. Mizutani, *J. Non-Cryst. Solids* **227&230**, 456 (1998).

¹²D. L. Williamson, A. H. Mahan, B. P. Nelson, and R. S. Crandall, *Appl. Phys. Lett.* **55**, 783 (1989).

¹³M. A. El Khakani, M. Chaker, A. Jean, S. Boily, H. Pépin, J. C. Kieffer, and S. C. Gujrathi, *J. Appl. Phys.* **74**, 2834 (1993).

¹⁴M. Fathallah, *J. Non-Cryst. Solids* **164&166**, 909 (1993).

¹⁵W. K. Choi, F. L. Loo, F. C. Loh, and K. L. Tan, *J. Appl. Phys.* **80**, 1611 (1996).

¹⁶M. P. Delplancke, J. M. Powers, G. J. Vandentop, M. Salmeron, and G. A. Somorjai, *J. Vac. Sci. Technol. A* **9**, 450 (1991).

¹⁷W. K. Choi, L. J. Han, and F. L. Loo, *J. Appl. Phys.* **81**, 276 (1997).

¹⁸D. Mencaraglia, K. S. Kim, E. Bardet, M. Cuniot, J. Dixmier, P. Elkaim, and E. Caristan, in *Proceedings of the 2nd World Conference and Exhibition on Photovoltaic Solar Energy Conversion*, edited by J. Schmidt, H. A. Ossensbrynck, P. Helm, H. Ehmann, and E. D. Dunlop (European Commission Joint Research Center, Vienna, 1998), pp. 1882–1885.

¹⁹F. Demichelis, G. Crovini, C. F. Pitti, E. Tresso, R. Galloni, R. Rizzoli, S. Summonte, F. Zignani, P. Rava, and A. Madan, *Philos. Mag. B* **69**, 377 (1994).

²⁰M. Fathallah, R. Gharbi, G. Crovini, F. Demichelis, F. Giorgis, C. F. Pirri, E. Tresso, and P. Rava, *J. Non-Cryst. Solids* **198&200**, 490 (1996).

²¹F. Demichelis, F. Giorgis, C. F. Pirri, and E. Tresso, *Philos. Mag. A* **72**, 913 (1995).

²²G. Ambrosone, S. Catalanotti, U. Coscia, S. Mormone, A. Cutolo, and G. Breglio, in *Proceedings of the 2nd World Conference and Exhibition on Photovoltaic Solar Energy Conversion* (Ref. 18), p. 770.

²³T. Datta and J. A. Woollam, *Phys. Rev.* **39**, 1953 (1989).

²⁴T. Datta, J. A. Woollam, and W. Notohamiprodjo, *Phys. Rev. B* **40**, 5956 (1989).

²⁵T. Datta, R. Noufi, and S. K. Deb, *Appl. Phys. Lett.* **47**, 1102 (1985).

²⁶A. Höfgen, V. Heera, F. Eichhorn, and W. Skorupa, *J. Appl. Phys.* **84**, 4769 (1998).

²⁷W. Beyer, H. Wagner, and H. Mell, in *Materials Issues in Applications of Amorphous Silicon Technology*, edited by D. Adler, A. Madan, and M. J. Thompson, *Mater. Res. Soc. Symp. Proc.*, No. 49 (Materials Research Society, Pittsburgh, 1985), p. 189.

²⁸W. Lin, H. K. Tsai, S. C. Lee, W. J. Sah, and W. J. Tzeng, *Appl. Phys. Lett.* **51**, 2112 (1987).